01 Jan 1993

Automatic Color Segmentation Algorithms-with Application to Skin Tumor Feature Identification

Scott E. Umbaugh

Randy Hays Moss
Missouri University of Science and Technology, rhm@mst.edu

William V. Stoecker
Missouri University of Science and Technology, wvs@mst.edu

G. A. Hance

Recommended Citation

S. E. Umbaugh et al., "Automatic Color Segmentation Algorithms-with Application to Skin Tumor Feature Identification," *IEEE Engineering in Medicine and Biology Magazine*, Institute of Electrical and Electronics Engineers (IEEE), Jan 1993.
The definitive version is available at https://doi.org/10.1109/51.232346

Automatic Color Segmentation Algorithms

With Application to Skin Tumor Feature Identification

Scott E. Umbaugh[1]
Randy H. Moss[2]
William V. Stoecker[3]
Gregory A. Hance[1]
[1]Department of Electrical Engineering
Southern Illinois University at Edwardsville
[2]Department of Electrical Engineering
University of Missouri-Rolla
[3]Department of Internal Medicine
University of Missouri-Columbia
Department of Computer Science
University of Missouri-Rolla
Stoecker and Associates

Two color-image segmentation methods have been developed. The first is based on a spherical coordinate transform of original RGB data. The second is based on a mathematically optimal transform, the principal components transform (also known as eigenvector, discrete Karhunen-Loevé, or Hotelling transform). These algorithms are applied to the extraction from skin tumor images of various features such as tumor border, crust, hair, scale, shiny areas, and ulcer. The results of this research will be used in the development of a computer vision system which will serve as the visual front-end of a medical expert system that will automate visual feature identification for skin tumor evaluation [1].

Materials and Methods

Equipment and Tools

Hardware: The images used in this research were digitized with a monochrome video camera, an NEC TI-23A CCD model, interfaced to a Gould DeAnza Image Processing System model IP8400, and a Digital Equipment Corporation VAX 11/780 minicomputer. Images were digitized from 35 mm color photographic slides obtained from a private dermatology practice and from New York University or, in one case, from a pamphlet obtained from the American Cancer Society. The digital images had a spatial resolution of 512×512 pixels, and a grey scale resolution of eight bits—256 levels.

The color images were obtained by digitizing the slide three times, each time using a different filter for each of the red, green, and blue planes. The filters used were broadband bandpass optical filters, with the red filter passing wavelengths in the 600 to 700 nm range, green the 500 to 600 nm range, and blue the 400 to 500 nm range. Kodak Wratten filters #29, #61, and #47 were used, in conjunction with #0 neutral density filters which were used to equalize the portions of red, green, and blue when digitizing white light.

Software: The software developed for this research was written in the C programming language on the VAX minicomputer, which was operating under the 4.3 BSD UNIX operating system. The C shell language was also used for batch files, which allowed for the processing of large blocks of images without user interaction. The 1st-Class Fusion [2] expert system development software was used as an automated induction engine for the development of classification rules.

As the target system for this development is a microprocessor-based system, there was a high degree of motivation to reduce the amount of data (each image is 0.75 Mbytes) to be processed, and to make the processing algorithms as efficient as possible. This was accomplished by such methods as color quantization to reduce color information, averaging to reduce spatial data, and generating program code that was as efficient as possible.

Feature Files

In addition to the digitized images, a database of feature information has been created by a dermatologist using software developed by the research team. This software allows the user to display an image and mark certain blocks (in this case 32×32 pixel blocks) as containing a specific feature. Through the use of these feature files, specific sections of an image may be selected for processing by the masking out of blocks within the image that are not of interest.

Feature masking served an important role in the development of the feature identification software modules in this project. With the feature marking software that was developed, the research team was able to proceed independently on each module. The development of the feature marking software, and the feature data base, proved its utility in the development of the software for this research. This model may be used for any large image processing/expert system project, as without it there would be no way to test each module independently, and much effort may be wasted enhancing modules that are already functioning properly.

In addition to using the feature files to mask out unwanted portions of the image, the feature files were used to obtain a success measure for the image segmentation algorithms developed. Each feature was marked on a block-by-block basis as either contain-

0739-5175/93/$3.00©1993

1a. Tumor image 50, the original.

1b. Tumor image 50, after PCT/median 3-D split (four colors).

1c. Tumor image 50, after SCT/center 2-D split (four colors).

ing the feature completely, marked as a full block, or containing the border of this feature, marked as a partial block. If the feature was not present in a given block, then nothing was marked for this feature in that block. Thus, the feature files provided a data base that could be used to test the success of a feature identification module and provided the necessary information to a module under development.

Induction Methods

Induction is the process of generating a general classification algorithm from a set of specific examples. It is a reasoning process that allows human beings to formulate theories from limited and specific experiences, that can then be used to predict future events [3]. In the context of this research, induction was used to generate a rule, based on color statistics, to determine the number of colors needed for the segmentation of a tumor image.

Heuristics: Heuristics are rules that human beings have developed as a direct result of their own experiences. These rules provide for the prediction of future events based on past experience. The induction mechanisms that are involved are not very well understood. In the development of an expert system, the expert is often called upon to provide heuristics to the system developer so that the experience of the expert can be codified. This process of translating the expert's knowledge into a formal system is usually the most difficult task facing the expert system developer.

Formal Induction Methods: The concept of machine intelligence is closely related to the concept of automatic learning [4]. In order for a machine to learn, it must be able to generate concepts and apply these concepts to new situations [3]. This is where formal, or automatic, induction methods are used.

Many of the formal induction methods that have been developed are based on first or higher order predicate calculus that has been extended to allow for inductive inferences. Some of these extensions are based on heuristics that human beings have applied effectively in specific domains. Some of these methods are known as interference matching, maximal unifying generalizations, conceptual clustering, and constructive induction [3].

Another general category of induction methods, currently the subject of much research, is neural networks. These approaches have their foundations in statistical analysis, through the use of discriminant functions, and are conceptually extended to first the perceptron [5] and then on to more complex neural net concepts. They are all based on the concept of finding the best set of coefficients, or weight vectors, that minimize a given error function.

The main unifying concept for all of the different induction methods is that they try to learn to classify input patterns into output patterns. The mechanism that was used in this research, as incorporated into the 1st Class Fusion [2] software, is based on an algorithm known as ID3. This algorithm generates decision trees that are based on the input example data [6]. These decision trees are then coded as rules in the C programming language and incorporated into the software that was developed to classify skin tumors and skin tumor features. ID3 was specifically designed to handle large masses of data while its processing time increases only linearly with the complexity of the problem [6]. This feature makes it feasible to use on a personal computer system.

Color Identification in Skin Tumors

Color Spaces and Transforms

A color space is a geometrical and mathematical representation of color. Most of the spaces reviewed here attempt to relate the way in which colors are defined to the way that humans perceive them [7]. There is no general method that has been developed that is applicable to all domains; the number of variables involved make the complexity of the problem such that, in most practical applications, a complete theoretical analysis is not feasible. In any problem of color quantification, the first step toward a solution is to define the color space.

The Original RGB Space: The original RGB (red, green, blue) color space was created by the digitizing of color slides using red, green, and blue filters and a monochrome video camera. This process generates a 3-D vector for each pixel, where each component has a value ranging from 0 to 255. This RGB color space was modeled mathematically by an orthogonal geometry. In this way a pixel can be represented by the vector consisting of its RGB component values or any linear, or non-linear, transformation of these values. All of the color spaces described below are mathematical transformations based on this original RGB data.

The Intensity/Hue/Saturation Transform: This transform is a simplified version of the Munsell system, which is based on human perception of color. The IHS (Intensity/Hue/Saturation) color space [8] is more useful to the engineer than the Munsell system, as it can be modeled mathematically in a reasonable form.

The I component, intensity, corresponds roughly to the brightness or amount of energy that is in the signal. The S component, saturation (Munsell uses the term chroma), measures the amount of white that is in the color. For example, pink is an unsaturated red—the more white that is added to the color the less saturated the color becomes. The H, hue, component is approximately proportional to the average wavelength of

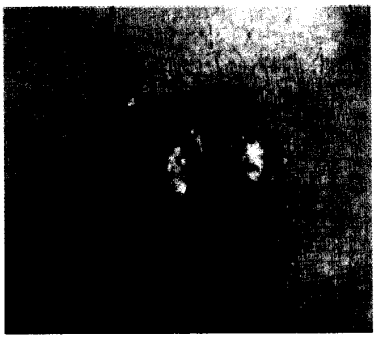

2a. Tumor image 30, the original.

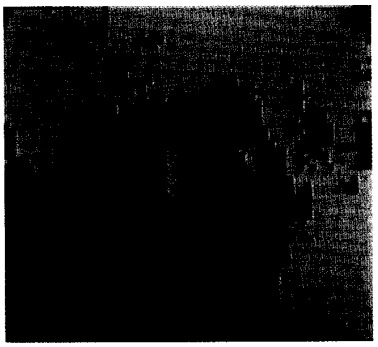

2b. Tumor image 30, after PCT/median 3-D split (four colors).

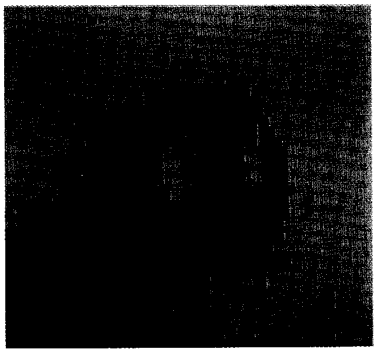

2c. Tumor image 30, after SCT/center 2-D split (four colors).

the color. Perceptually, hue is what people normally think of when the term "color" is used; that is, it can be described by words such as blue, red, or yellow.

The Spherical Transform: This transform was originally defined as part of a color segmentation method developed to identify variegated coloring in skin tumor images [7]. This transformation splits the color space into a two-dimensional color space, represented by the two angles, Angle A and Angle B; and a one-dimensional intensity (brightness) space represented by the vector length L.

Chromaticity Coordinates: Chromaticity coordinates can be defined in terms of the original RGB vectors [9], or another color space may be used as a basis. However, the resulting chromaticity coordinates are most useful for linear, as opposed to non-linear, transforms of the RGB data. Basically, the chromaticity coordinates are color component values that have been normalized to the intensity vector.

The CIE Transforms: The CIE transform [9] provides an international standard for the quantification of color. In the standard CIE color space, first developed in 1931, the coordinate system used is referred to as the 1931 CIE XYZ space. The standard transform between the CIE XYZ space and another 3-dimensional color space, such as the original RGB space, can be defined by a linear transform [10].

An alternative to the standard CIE transform is the uniform color transform designated 1976 CIE L*u*v*, also called CIE LUV [9]. This color space is defined in a way so that two color vectors that are equally spaced in the color space are also equally spaced on a perceptual basis; this is not true for other color space definitions.

Image Segmentation by Color Information

Image segmentation is important in many computer vision and image processing applications. Division of the image into regions corresponding to objects of interest is necessary before any processing can be done at a level higher than that of the pixel. Identification of real objects, pseudo-objects, shadows, or actually finding anything of interest within the image requires some form of segmentation.

The Segmentation Algorithms

Spherical Coordinate Transform/Center 2-D Split: This algorithm, SCT/Center 2-D Split, was initially developed for the identification of variegated coloring [11]. This algorithm consists of transforming the original RGB data into a spherical transform domain that consists of a two-dimensional color space represented by two angles, Angle A and Angle B, and a one-dimensional intensity space. The two-dimensional color space is then divided using a center split [7].

Principal Components/Median 3-D Split: This color segmentation algorithm was developed since, in some cases, the results provided by the SCT/Center 2-D algorithm were not totally satisfactory [16]. This algorithm is based on the principal components transform [12,17]. The median 3-D split component of the segmentation method is based on an algorithm that was developed for color compression; specifically, to map 24-bit-per-pixel color images into images requiring an average of two bits per pixel [13, 14]. As with the previously defined color segmentation method, the image is preprocessed by block averaging and feature masking [7].

The Principal Components Transform: The principal components transform (PCT) is based on statistical properties of the image. Classically, in image processing, the PCT is applied to the two-dimensional image domain. In this case, the PCT is applied to the three- dimensional color space. It was believed that the PCT used in conjunction with the median split algorithm would provide a satisfactory color image segmentation, since the PCT aligns the main axis along the maximum variance path in the data set; for feature selection in pattern recognition theory, a feature with large variance is said to have large discriminatory power [15].

The PCT is often used in image compression (coding), since this transform is optimal in the least-square-error sense [12]. What this means is that most of the information, here information is assumed to be directly correlated with variance, is in a reduced dimensionality. In the case of the skin tumor images, it was experimentally determined that the dimension with the largest variance after the PCT was performed contained approximately 91 percent of the variance. (If used for compression this would allow at least a 3:1 compression and still retain 91 percent of the information.)

In order to find the PCT for a given image, the three- dimensional color covariance matrix must first be found. This covariance matrix is defined as follows (the following equations assume the original space is RGB space, but any 3-D color space can be used):

$$[\,COV\,]_{RGB} = \begin{bmatrix} C_{RR} C_{GR} C_{BR} \\ C_{RG} C_{GG} C_{BG} \\ C_{RB} C_{GB} C_{BB} \end{bmatrix}$$

where

$$C_{RR} = \frac{1}{N} \sum_{i=1}^{N} (\,R_i - \mu_R\,)^2$$

and

3a. Tumor image 13, the original.

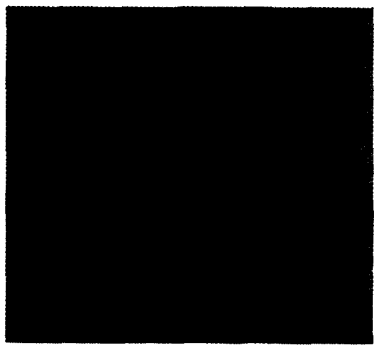

3b. Tumor image 13, after PCT/median 3-D split (four colors).

3c. Tumor image 13, after SCT/center 2-D split (four colors).

$$\mu_R = \frac{1}{N}\sum_{i=1}^{N} R_i$$

and

N = number of pixels in the image

R_i = red component of the i^{th} pixel

μ_R = mean of all the red pixel components

Similar equations are used for the other autocovariance variables, C_{GG} and C_{BB}. The cross-covariance terms, C_{GR}, C_{BR}, C_{RG}, C_{BG}, C_{RB}, C_{GB}, are defined as follows:

$$C_{XY} = \frac{1}{N}\left[\sum_{i=1}^{N} X_i Y_i\right] - \mu_X \mu_Y$$

with the means defined as before.

Now it can be shown that if the eigenvectors of the covariance matrix are used as a linear transform matrix on the original [R G B] vectors, then the resulting vectors have components that are uncorrelated [12]. Geometrically, this means that the primary axis has been aligned where the variance in the data is maximal. The new vectors, here called $[X_1\ X_2\ X3]^T$, are obtained by this equation:

$$\begin{bmatrix} X_1 \\ X_2 \\ X_3 \end{bmatrix} = \begin{bmatrix} E_{11}E_{12}E_{13} \\ E_{21}E_{22}E_{23} \\ E_{31}E_{32}E_{33} \end{bmatrix} \cdot \begin{bmatrix} R \\ G \\ B \end{bmatrix}$$

where [E_{11} E_{12} E_{13}], [E_{21} E_{22} E_{23}], and [E_{31} E_{32} E_{33}] are the eigenvectors of the covariance matrix.

It was experimentally determined that, for this domain of skin tumor images, the X_i component obtained from the eigenvector corresponding to the largest eigenvalue contained approximately 91 percent of the variance, the X_i component obtained from the eigenvector corresponding to the second largest eigenvalue contained approximately 6 percent of the variance, and the X_i component obtained from the eigenvector corresponding to the smallest eigenvalue contained approximately 3 percent of the variance.

Median Split: Once the PCT has been performed on the image data, the color space segmentation scheme is performed. This median split method works by first finding the axis that has the maximal range. Then, the data are divided along this axis, where there are equal numbers of points on either side of the split—the median point. This process continues until the desired number of colors is reached. At this point, averages are calculated for all the pixels falling within a single parallelepiped. Then, each pixel is mapped to the closest average color values, based on a Euclidean distance measure [13, 14].

Application of Color Segmentation to Feature Extraction

Color Segmentation Results on Six Features

The six features that were selected for this study were tumor, crust, hair, scale, shiny and ulcer. These features were initially included in the feature files, since the dermatologist believed this set of six to be the most important in the automatic diagnosis of skin tumors. These features were all marked in the feature files on a set of 500 tumor images, of which 57 contained crust, 70 contained hair, 89 contained scale, 88 contained shiny areas, and 36 were marked as containing ulcer.

Ulcer can be visually defined as a dark red area within the tumor border. Ulcer objects are usually round, and may have fuzzy or irregular borders. The shiny feature is defined by an area in the image that reflects light well—normally appearing white compared to the surrounding area. Scale consists of upturned, ivory-colored pieces of dead skin. Crust is dried blood or serum within the tumor border, commonly called scabs.

Crust and scale exhibit a rough texture, whereas ulcer and shiny appear smooth. Hair can be identified by finding abrupt edges that define a long, thin object. The tumor itself can be defined by color, texture, three-dimensional shape, or any combination of these three attributes. In some of the tumors, the boundary is so vague that even the dermatologist had difficulty finding the tumor border within the image.

Since many of these features require more than the color attribute to be identified, a success measure for the color segmentation had to be defined. The feature files contained the necessary information, as both full blocks and partial blocks were marked for each feature. The feature blocks that were marked as partial were the places in the image where the borders for each feature existed. Thus, a success measure for the color segmentation was defined, and this measure was independent of any feature extraction modules that may be used in further processing.

Success Measure: The success measure was defined by three metrics: direct hits, near hits, and total hits. A direct hit was counted if a color change existed in the segmented image in a partial block, and a near hit was counted if a color change was found within a half block of a partial block. Total hits were simply the sum of the direct hits and the near hits. Since each tumor and each feature may have had a different number of potential hits, i.e., partial blocks, the metrics are presented as percentages of the total number of partial blocks for that particular feature. Of course, this measure is meaningful only if the segmentation is representative of the original image—randomly distributed pixel values may provide 100 percent success by this measure. Also, these

metrics are only of interest for small numbers of colors.

Both of these constraints were met. The color segmentation methods provided results that were highly correlated to the original data, and the maximum number of colors used was ten. The high correlation to the original data was determined both by visual observation of some of the segmented images (see Figs. 1-3) and by the fact that both segmentation algorithms are adaptive to the image data itself. The PCT, with its reliance on both first and second order statistics, provides a segmentation that is highly dependent on the original image data.

Experimental Methodology: The SCT/2-D programs were constrained to the number of colors being a perfect square. Therefore, four and nine colors were selected for the application of this segmentation method. The PCT/3-D programs were more versatile and the experiment was run varying the number of colors from two through ten. Also, the PCT method was not defined for a specific color space transform, so six different color space transforms were utilized. These six were: RGB, IHS, spherical transform, chromaticity coordinates (on RGB), CIE XYZ, and CIE LUV.

The PCT segmentation method also allowed for the implementation of a program that would vary the number of colors that the image was segmented into based on image statistics. Using the AI induction engine [2], and a training set of 30 examples, a rule was defined for splitting the image into two, three, four, or five colors based on first and second order RGB statistics. The number of colors utilized as the "correct" number in the training set was determined by the dermatologist based on the information that he thought was important for diagnosis.

Results: The results of the two color space segmentation methods are illustrated in Figs. 1-3. Figures 1a, 2a and 3a illustrate

Table 1. PCT segmentation results using the AI-induced rule to determine the number of colors for segmentation—Tumor

Color Space Transform	Average Direct Hits	Average Near Hits	Average Total Hits
CHR	88.1%	10.8%	98.9%
XYZ	83.1%	13.7%	96.8%
LUV	85.4%	13.1%	98.5%
IHS	83.1%	13.6%	96.7%
RGB	82.6%	14.3%	97.0%
SPH	83.4%	13.9%	97.3%

Table 2. PCT segmentation results using the AI-induced rule to determine the number of colors for segmentation—Crust

Color Space Transform	Average Direct Hits	Average Near Hits	Average Total Hits
CHR	91.6%	7.7%	99.3%
XYZ	77.4%	17.0%	94.4%
LUV	88.1%	10.6%	98.7%
IHS	82.5%	15.3%	97.8%
RGB	78.7%	16.9%	95.5%
SPH	79.5%	17.1%	96.6%

Table 3. PCT segmentation results using the AI-induced rule to determine the number of colors for segmentation—Hair

Color Space Transform	Average Direct Hits	Average Near Hits	Average Total Hits
CHR	78.5%	15.4%	93.8%
XYZ	75.5%	17.7%	93.2%
LUV	74.7%	17.5%	92.3%
IHS	70.7%	20.6%	91.4%
RGB	73.2%	18.8%	92.0%
SPH	73.7%	18.3%	92.0%

Table 4. PCT segmentation results using the AI-induced rule to determine the number of colors for segmentation—Scale

Color Space Transform	Average Direct Hits	Average Near Hits	Average Total Hits
CHR	88.4%	9.9%	98.3%
XYZ	80.4%	16.4%	96.8%
LUV	82.7%	14.1%	96.8%
IHS	81.9%	15.7%	97.6%
RGB	77.4%	17.6%	95.0%
SPH	76.9%	17.9%	94.8%

Table 5. PCT segmentation results using the AI-induced rule to determine the number of colors for segmentation—Shiny

Color Space Transform	Average Direct Hits	Average Near Hits	Average Total Hits
CHR	87.9%	10.1%	98.0%
XYZ	85.7%	11.6%	97.3%
LUV	89.1%	8.7%	97.8%
IHS	84.7%	12.6%	97.2%
RGB	83.0%	13.6%	96.6%
SPH	81.5%	14.2%	95.7%

Table 6. PCT segmentation results using the AI-induced rule to determine the number of colors for segmentation—Ulcer

Color Space Transform	Average Direct Hits	Average Near Hits	Average Total Hits
CHR	87.7%	11.5%	99.2%
XYZ	79.0%	16.7%	95.7%
LUV	85.6%	13.3%	98.9%
IHS	88.1%	9.6%	97.7%
RGB	87.0%	10.2%	97.2%
SPH	84.9%	12.3%	97.2%

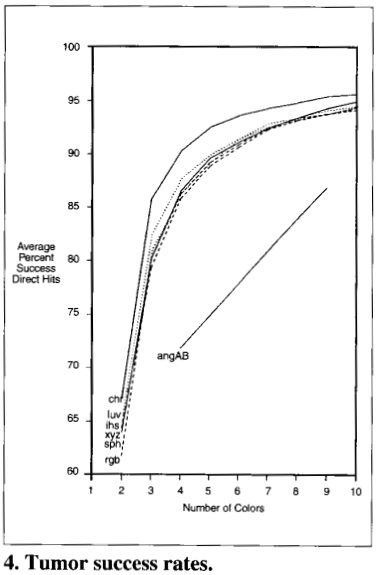

4. Tumor success rates.

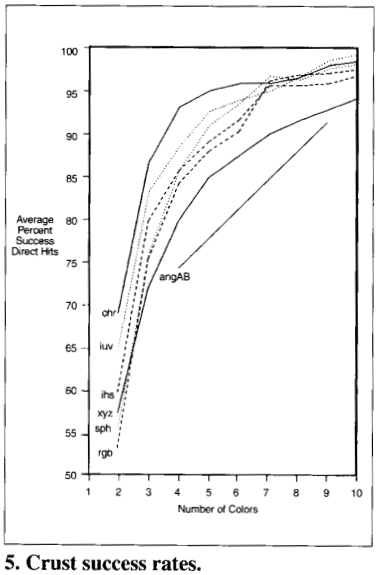

5. Crust success rates.

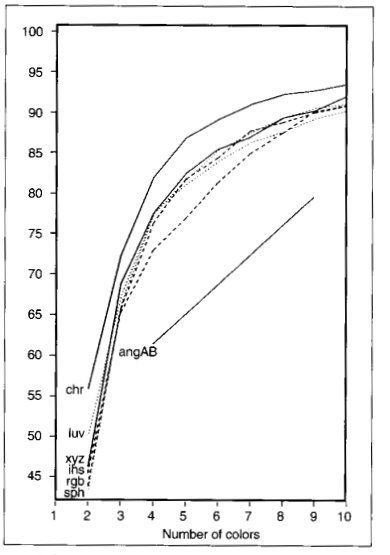

6. Hair success rates.

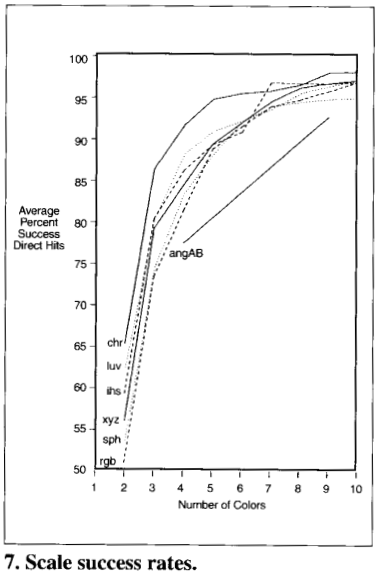

7. Scale success rates.

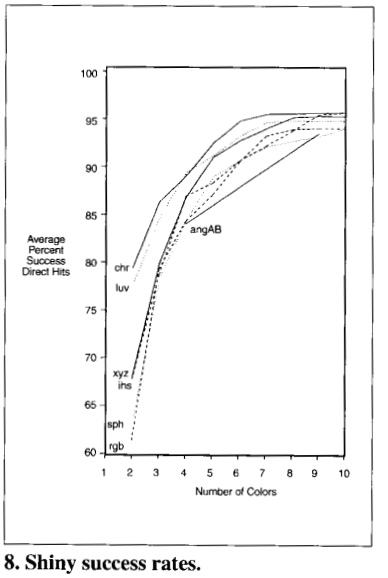

8. Shiny success rates.

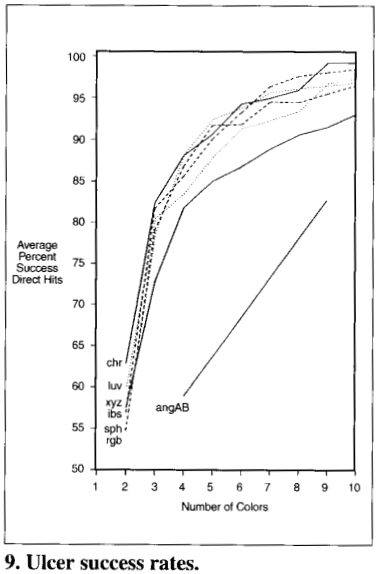

9. Ulcer success rates.

three skin tumor images, numbered 50, 30 and 13 respectively, that exhibit several tumor features such as variegated coloring, ulcer, shiny and crust. Before applying each segmentation algorithm a preprocessing measure was taken to average the original 512×512 images over an 8×8 pixel block to reduce spatial data for faster processing and decrease the effects of noise.

Figures 1b, 2b and 3b show the results of applying the PCT/Median 3-D split to each of the three original tumor images after being mapped to chromaticity coordinates. Figures 1c, 2c and 3c illustrate the results of applying the SCT/Center 2-D split to each of the three original tumor images in the RGB space.

In both algorithms, the image was segmented into four colors and then mapped back to the RGB space using the mean value of each segmented region with respect to the original tumor image. All of the images were then once again enlarged back to their original size of 512×512 using pixel replication.

Overall the best results were obtained from the PCT/Median 3-D split algorithm. This can be seen by the accuracy in which this algorithm segmented out the ulcerated areas of tumor images 30 and 13; these areas appear as saturated red regions in Figs. 2b and 3b. The algorithm also did a better job of segmenting out the crust feature present in tumor image 50; this feature appears as a dark saturated red region in Fig. 1b. Both algorithms were accurate at separating the shiny, reflective areas of images 30 and 13 from the rest of the tumor and appear as the same color as the skin in Figs. 2b, 2c, 3b and 3c. In addition to demonstrating their success as segmentation methods for the identi-

fication of these features, both algorithms also proved to be useful in detecting tumor borders [16].

The results obtained from the AI-induced rule to determine the number of colors can be found in Tables 1 through 6. These resulted from the use of the PCT/3-D Median Split algorithm and it should be noted that preliminary experimentation indicated that using the median split algorithm, without the PCT being performed first, provided results that were from approximately 5 percent to 15 percent lower than using it in conjunction with the PCT [1].

The most significant results were obtained from the success on the tumor itself, since this test set was the largest set—500 images. Overall, the chromaticity coordinate color space provided the best results, with the highest percentage of total hits on all six features, and the highest percentage of direct hits on all but shiny and ulcer, where other color spaces showed marginally better success. It should be noted that these metrics are averages and large variances in the data preclude definitive statistical comparisons. However, based on results presented here and elsewhere [1] it appears that the chromaticity transform shows the most promise.

The results from using a fixed number of colors is contained in the following plots and tables. The plot for tumor success rates, direct hits, is given in Fig. 4. Here, the line labeled angAB refers to the SCT/2-D Center Split color segmentation algorithm, due to its reliance on the two-dimensional space defined by Angle A and Angle B. All the other plots are obtained using the PCT/3-D Median Split color segmentation algorithm, where the label refers to the specific color space utilized.

The chromaticity coordinate transform, chr, is shown to have the greatest success across the entire range of number of colors. The CIE LUV transform has the second highest success rate with two to eight colors. At the eight-color point, the CIE XYZ transform surpasses the LUV transform. The SCT/2-D Center Split method is shown to be inferior to the PCT/3-D Median Split across the entire range of number of colors and for any of the color spaces.

Figures 5 through 9 illustrate similar success for crust, hair, scale, shiny and ulcer. In all of these, the PCT/3-D Median Split is shown to be superior to the SCT/2-D Center Split algorithm. The chromaticity coordinate transform shows the greatest success for most of these features, especially for smaller numbers of colors. The best success for smaller numbers of colors is important, as it will be easier to obtain success with the feature extraction modules if the image contains minimal information.

It can be seen in all the plots that the success measure levels off after about five or six colors. In most cases the success for direct hits approaches about 95 percent at the six-color point. After the image segmentation, the feature extraction modules will be needed to identify the specific border for each feature. If the feature extraction modules can approach the 95 percent success level provided by the segmentation method, then all these features will be identified satisfactorily.

Conclusions

This research has demonstrated the importance of color information for the automatic diagnosis of skin tumors by computer vision. The feature file paradigm was shown to provide an efficacious methodology for the independent development of software modules for expert system/computer vision research. The automatic induction tool was used effectively to generate a rule to select number of colors for segmentation.

Of the two color image segmentation algorithms that were developed, the PCT/Median 3-D Split was shown to be superior to the SCT/Center 2-D Split. The PCT/Median 3-D Split color segmentation method was used to segment images for the extraction of the features ulcer, crust, scale, shiny, tumor and hair. These results illustrated that when the images were segmented into six or more colors, about 95 percent success was achieved regarding color changes in the corresponding border blocks for all six features. The chromaticity coordinate transform color space provided the optimal results. With the AI induced rule for deciding how many colors to segment an image into based on color statistics, the chromaticity transform also provided the best results.

Acknowledgement

This work was supported in part by a National Science Foundation Small Business Innovation Research Grant, ISI #8521284, a Funded University Research Grant, #F-EN310, and a Fourth Quarter Research Fellowship Grant from Southern Illinois University at Edwardsville.

Scott E. Umbaugh is currently an assistant professor in electrical engineering at Southern Illinois University at Edwardsville. He received the BSE degree from SIUE in 1982, the MSEE from the University of Missouri-Rolla in 1987, and the Ph.D. in electrical engineering from UMR in 1990. Umbaugh worked as a computer software/hardware engineer for ITT North Electric in Columbus, Ohio, and McDonnell Douglas Corp. and Affinitec Corp. in St. Louis from 1981 through 1986. He currently serves on the editorial board of the *IEEE Engineering in Medicine and Biology Magazine* and the *Pattern Recognition Journal*. He is a member of the IEEE Education Society, the IEEE Engineering in Medicine and Biology Society, the Pattern Recognition Society, the American Society for Engineering Education, and Sigma Xi. **Dr. Umbaugh can be reached at the Department of Electrical Engineering, Southern Illinois University at Edwardsville, Edwardsville, IL, 62026-1801, or by e-mail at: seu@minuet.siue.edu.**

Randy H. Moss received the BSEE and MSEE from the University of Arkansas and the Ph.D. from the University of Illinois. He is currently Professor of Electrical Engineering at the University of Missouri-Rolla. He has developed a machine vision course and laboratory at the University of Missouri-Rolla under a grant from the General Electric Foundation.

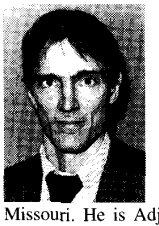

William V. (Van) Stoecker received the B.S. degree in mathematics in 1968 from the California Institute of Technology, the M.S. in systems science in 1971 from the University of California, Los Angeles, and the M.D. in 1977 from the University of Missouri. He is Adjunct Assistant Professor of Computer Science at the University of Missouri-Rolla and Clinical Assistant Professor of Internal Medicine-Dermatology at the University of Missouri-Columbia.

Gregory A. Hance is currently a research assistant in electrical engineering at Southern Illinois University at Edwardsville. He received the BSE degree from SIUE in 1991, and the MSEE degree from SIUE in 1993. He is a member of the IEEE Computer, Signal Processing and Engineering in Medicine and Biology societies.

References

1. **Umbaugh SE:** Computer Vision in Medicine: Color Metrics and Image Segmentation Methods for Skin Cancer Diagnosis, PhD Dissertation, Electrical Engineering Dept, Univ of Missouri-Rolla. UMI Dissertation Services, Ann Arbor, MI, 1990.

2. **Thomas W, Hapgood W:** *1st-Class Fusion*, 1st-Class Expert Systems Inc., Wayland, MA, 1987.

3. **Genesereth MR, Nilsson NJ:** *Logical Founda-*

tions of Artificial Intelligence, Morgan Kaufman, Palo Alto, CA, 1988.

4. **Tanimoto SL:** *The Elements of Artificial Intelligence*, Computer Science Press, Rockville, MD, 1987.

5. **Devijver PA, Kittler J:** *Pattern Recognition: A Statistical Approach*, Prentice-Hall International, London, 1982.

6. **Quinlan JR:** Learning efficient classification procedures and their application to chess end games. In: Michalski RS, Carbonell J, Mitchell TM (Eds.): *Machine Learning: An Artificial Intelligence Approach*, Morgan Kaufman, Los Altos, CA, 1983.

7. **Umbaugh SE:** Computer Vision in Medicine: Identification of Variegated Coloring in Digitized Skin Tumor Images, MS Thesis, Electrical Engineering Dept, Univ of Missouri-Rolla, 1987.

8. **Ballard DH, Brown CM:** *Computer Vision*, Prentice-Hall, Englewood Cliffs, NJ, 1982.

9. **Wyszecki G, Stiles WS:** *Color Science: Concepts, and Methods, Quantitative Data and Formulae*, John Wiley and Sons, New York, 1982.

10. **Wasserman GS:** *Color Vision: An Historical Introduction*, John Wiley and Sons, New York, 1978.

11. **Umbaugh SE, Moss RH, Stoecker WV:** Automatic color segmentation of images with application to detection of variegated coloring in skin tumors. *IEEE Engng Med Biol* 8(4):43-52, Dec 1989.

12. **Gonzalez RC, Wintz P:** *Digital Image Processing*, Addison-Wesley Publishing, Reading, MA, 1987.

13. **Heckbert P:** Color image quantization for frame buffer display. *Comput Graph*, 16(3):297-304, 1983.

14. **Campbell G, DeFanti TA, Frederiksen J, Joyce SA, Leske JA, et al:** Two bit/pixel full color encoding. *Siggraph* 20(4), 1986.

15. **Ohta YI, Kanade T, Sakai T:** Color information for region segmentation. *Comput Graph and Image Processing* 13:222-241, 1980.

16. **Umbaugh SE, Moss RH, Stoecker WV:** An Automatic Color Segmentation Algorithm with Application to Identification of Skin Tumor Borders. *Comput Med Imaging and Graph* 13(3):227-235, May-Jun, 1992.

17. **Pratt WK:** *Digital Image Processing*, 2nd Ed, John Wiley and Sons, New York, 1991.

Facial Communications

(continued from page 48)

of the eigenvectors. Additionally, the proliferation of high definition television (HDTV) and video phone technology has prompted the creation of low cost DCT chips [2]. Both techniques are relatively simple to implement and, most importantly, can be readily customized to the unique needs of the subject.

Steven K. Rogers is Professor in the Department of Electrical and Computer Engineering at the Air Force Institute of Technology, Wright-Patterson Air Force Base, Dayton, Ohio. He holds a Ph.D. and the rank of major in the U.S. Air Force and is presently conducting an extensive research program on optical information processing and neural networks. The research program addresses the problems inherent in making smart computers. **He can be reached at AFIT/EN, WPAFB, OH 45433-6583; email: rogers@afit.af.mil**

Pedro F. Suarez obtained his B.S. degree in electrical engineering from the U.S. Air Force Academy (1986) and his M.S. in electrical engineering from the Air Force Institute of Technology (1991). He is currently a captain in the U.S. Air Force and is stationed in California.

James R. Goble joined the U.S. Air Force in 1975, received his B.S. degree in electrical engineering from Ohio University, and was commissioned through OTS in 1986. He completed a tour at Fort Meade, Md., before entering the Masters Program in the School of Engineering, Air Force Institute of Technology, in June 1990. He is currently assigned to Los Angeles Air Base, California.

Dennis W. Ruck is Assistant Professor of Electrical Engineering at the Air Force Institute of Technology, Wright-Patterson Air Force Base, Dayton, Ohio. He received his Ph.D. from the Air Force Institute of Technology in 1990. Dr. Ruck has published over 30 articles on pattern recognition, artificial neural networks, and signal processing. He is a captain in the U.S. Air Force and chairman of the SPIE Conference on the Science of Artificial Neural Networks for 1993.

Craig Arndt received a B.S. in electrical engineering from Ohio State University in 1982, an M.S. in systems engineering and an M.S. in human factors engineering in 1989 and 1991, respectively, from Wright State University. He joined the U.S. Air Force in 1985 as a project engineer and moved to the Armstrong Lab in 1989 as a research engineer. He now heads the autolandmarking project. His current research interest include neural networks, signal processing, and face recognition.

Dr. Matthew Kabrisky is currently Professor Emeritus of Electrical Engineering, School of Engineering, Air Force Institute of Technology. His academic education includes a B.S. and M.S. from Polytechnic Institute of Brooklyn (1951 and 1952), and a Ph.D. in electrical engineering from the University of Illinois (1964). He has been a member of the faculty of the Air Force Institute of Technology since February, 1961. His current research involves the application of signal processing techniques to Air Force problems in autonomous weapons, motion sickness, and face recognition for access security.

References

1. **Suarez PF:** Face Recognition with the Karhunen-Loève Transform. Master's thesis, Air Force Institute of Technology, Dec 1991.

2. **Goble JR:** Face Recognition Using the Discrete Cosine Transform. Master's thesis, Air Force Institute of Technology, Dec 1991.

3. **Gonzalez R, Wintz P:** *Digital Image Processing*, Addison-Wesley Publishing, Reading, MA, 1987.

4. **Kreysig E:** *Advanced Engineering Mathematics*, John Wiley and Sons, New York, 1983.

5. **Turk MA, Pentland AP:** Recognition in face space. In: *Proc SPIE Intelligent Robots and Computer Vision IX: Algorithm and Techniques*, pp 43-54, 1990.

6. **Ahmed N, Rao K:** Discrete cosine transform. *IEEE Trans Computers*, pp 90-93, Jan 1974.

7. **Shanmugan KS:** Comments on the discrete cosine transform. *IEEE Trans Computers*, p 759, Jul 1975.

8. **Ang P:** Video compression makes big gains. *IEEE Spectrum*, pp 16-19, Oct 1991.

9. **Tou JT, Gonzalez R:** *Pattern Recognition Principles*, Addison-Wesley Publishing, Reading, MA, 1974.